

Benzenamine derivative as corrosion inhibitor of carbon steel in hydrochloric acid solution: Electrochemical and theoretical studies

M. Hayaoui^{1,3}, M. Drissi², M. Fahim², R. Salim^{1,3}, Z. Rais¹, S. Mouffarih¹,
M. Filali Baba¹, F. El Hajjaji¹, A. Zarrouk⁴, M. Taleb¹

¹ Laboratory of Engineering, Electrochemistry, Modeling and Environment (LIEME), Faculty of Sciences, University Sidi Mohamed Ben Abdellah, Fez, Morocco

² Laboratory of Materials Chemistry and Bio-technology of Naturals Products, Faculty of Sciences, University Moulay Ismail, Meknes, Morocco

³ Laboratory of separation processes, Faculty of Science, University Ibn Tofail, Kenitra, Morocco

⁴ LC2AME-URAC 18, Faculty of Science, First Mohammed University, PO Box 717, M-60 000 Oujda, Morocco.

Received 13 Jan 2017
Revised 05 Mar 2017
Accepted 07 Mar 2017

Keywords

✓ Carbon steel,
✓ HCl,
✓ Corrosion inhibition,
✓ Electrochemical techniques
✓ DFT
el.hajjajifadoua25@gmail.com

Abstract

N-(1-(propionyloxy) propylidene) benzenamine (PPB) was tested as corrosion inhibitor for carbon steel in 1M HCl by using polarization and electrochemical impedance spectroscopy (EIS) at 298-328 K. Then the experimental results were confirmed by theoretical calculations using DFT at B3LYP/6-31G (d, p) level of theory. The inhibition efficiency was found to increase with increase in PPB concentration but decreased with temperature. Activation parameters and Gibbs free energy for the adsorption process were calculated and discussed. It was found that PPB behaved as a mixed type inhibitor. The adsorption process of inhibitor obeyed the Langmuir isotherm. Impedance measurements showed that the double-layer capacitance decreased and charge-transfer resistance increased with increase in the inhibitor concentration and hence increasing in inhibition efficiency.

1-Introduction

Acid solutions are vastly used in the industry especially hydrochloric acid (HCl), the main applications domains are stripping, cleaning, elimination of localized deposits and descaling the metallic installation [1-3]. As consequences, the damages caused by application of this acid are not only the high cost for inspecting, repairing and replacement but contain also a public risk [4]. Working with this aggressive solution has led us to use corrosion inhibitors to limit their attack of different materials. In order to reduce the degradation of materials several methods of protection have been implemented. At present, many researches will develop using organic inhibitors. Particularly who's containing unsaturated bonds and / or heteroatom such as nitrogen, oxygen, and sulphur [5-20]. Therefore the effectiveness of inhibition increase with decreasing electronegativity of these functional atoms following this order $O < N < S < Se < P$. Often, other factors such as the structure of the molecule and more particularly the steric effects influence the adsorption of organic molecules [21].

The present paper explores the use of benzenamine derivative as corrosion inhibitor for carbon steel surface in hydrochloric acid solution using potentiodynamic polarization and electrochemical impedance spectroscopy methods. The effect of temperature on corrosion and inhibition processes are thoroughly assessed and discussed. Thermodynamic parameters governing the activation process were also calculated and discussed. Quantum chemical study using density functional theory (DFT) was further employed in an attempt to correlate the inhibitive effect with the molecular structure of N-(1-(propionyloxy) propylidene) benzenamine (PPB). The chemical structure of the studied (PPB) is given in Fig 1.

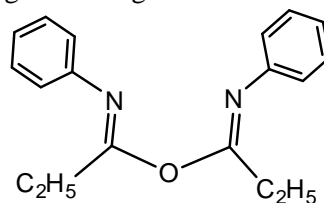


Figure 1: Chemical structure of N-(1-(propionyloxy) propylidene) benzenamine (PPB).

2. Experimental part

2.1. Materials

The steel used in this study is a carbon steel (CS) with a chemical composition (in wt%) of 99.21% Fe, 0.38% Si, 0.21% C, 0.05 %Mn, 0.05% S, 0.09% P and 0.01% Al.

2.2. Solutions

The aggressive solutions of 1M HCl were prepared by dilution of analytical grade 37% HCl with distilled water. The concentration range of N-(1-(propionyloxy) propylidene) benzenamine (PPB) used was 10^{-6} M to 10^{-3} M.

2.3. Electrochemical measurements:

Electrochemical experiments were recorded by using a Radiometer analytical (Voltalab-PGZ 301), coupled to a computer equipped with a software Voltmaster 4. The electrolysis cell was Pyrex of cylinder closed by cap containing five openings. Three of them were used for the electrodes. The working electrode was carbon steel with the value surface area adjacent of 1 cm^2 . Before each experiment, the electrode was polished using emery paper until 1200 grade. After this, the electrode was cleaned ultrasonically with distillate water. A saturated calomel electrode (SCE) was used as a reference. All potentials were given with reference to this electrode. The counter electrode was a platinum plate of surface area of 1 cm^2 .

2.3.1. Impedance spectroscopy measurements:

The electrochemical impedance spectroscopy measurements were carried out using a transfer function analyzer (Analytical Radiometer PGZ 301), with a small amplitude ac. Signal (10 mV), over a frequency domain from 100 KHz to 10 mHz at 298 K and an air atmosphere. The transfer charge resistance R_{ct} is obtained from the diameter of the semicircle in Nyquist representation. In this case, the inhibition efficiency is calculated using the following equation (1):

$$\eta_z \% = \frac{R_{ct}^i - R_{ct}^{\circ}}{R_{ct}^i} \times 100 \quad (1)$$

where, R_{ct}° and R_{ct}^i are the charge transfer resistance in absence and in presence of inhibitor, respectively.

2.3.2. Polarization measurements:

All potentials were given with reference to the saturated calomel electrode (SCE). The counter electrode was platinum. The working electrode was immersed in test solution during 30 min until a steady state open circuit potential (E_{corr}) was obtained. The polarization curve was recorded by polarization from -700 mV to -200 mV under potentiodynamic conditions corresponding to 1 mV/s (sweep rate) and under air atmosphere. Inhibition efficiency was calculated using Equation (2):

$$\eta_{\text{Tafel}} \% = \frac{I_{\text{corr}}^{\circ} - I_{\text{corr}}^i}{I_{\text{corr}}^{\circ}} \times 100 \quad (2)$$

where, I_{corr}° and I_{corr}^i are the corrosion current density in absence and presence of inhibitor, respectively.

2.6. Quantum chemical calculations:

Quantum chemical calculations were performed to clarify the correlation between the molecular structure of the inhibitor and its efficiency using the DFT at B3LYP/6-31G (d, p) level of theory by the Gaussian 09 program [22,23]. This approach is widely used in the analysis of the characteristics of the corrosion process. The following chemical quantum parameters were appreciated from the optimized molecular structure: the energy of the highest occupied molecular orbital (E_{HOMO}), the energy of the lowest unoccupied molecular orbital (E_{LUMO}), the energy band gap ($\Delta E_{\text{gap}} = E_{\text{HOMO}} - E_{\text{LUMO}}$), the electron affinity (A), the ionization potential (I), the dipole moment (μ) and the number of transferred electrons (ΔN).

3. Results and discussion:

3.1. Potentiodynamic polarization

3.1.1. Effect of concentration

Fig. 2 illustrates the potentiodynamic polarisation curve of carbon steel in 1M HCl solutions in the absence and presence of various concentrations of the PPB compound. The Electrochemical parameters such as corrosion potential (E_{corr}), corrosion current density (I_{corr}), Tafel cathodic slope (β_c) and inhibition efficiency values

(η_{Tafel} %) are given in Table 1. The potentiodynamic curves show that there is a clear reduction of both the anodic and cathodic currents in the presence of PPB compared with those for the blank solution.

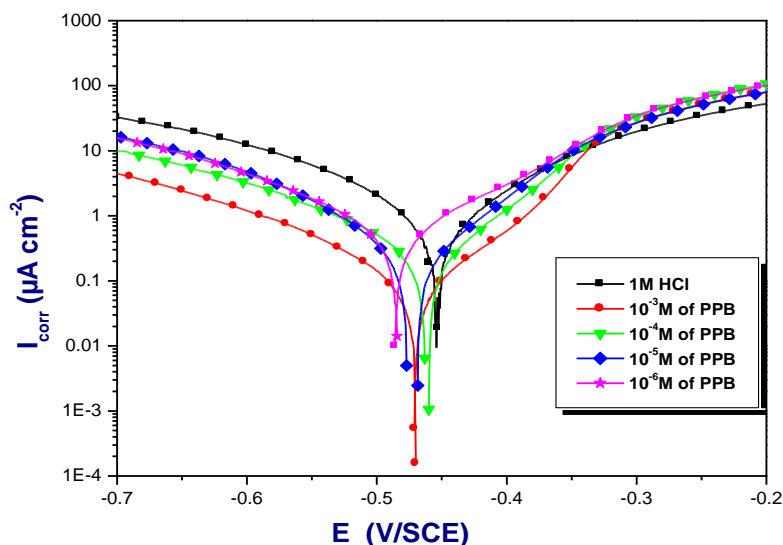


Figure 2: Polarization curve for carbon steel in 1M HCl containing different concentrations of PPB at 298K.

Table 1: Polarization parameters and the corresponding inhibition efficiencies for steel in 1M HCl containing various concentrations of PPB at 298 K.

Medium	Conc (M)	$-E_{\text{corr}}$ (mV/SCE)	I_{corr} ($\mu\text{A cm}^{-2}$)	$-\beta_c$ (mV dec^{-1})	η_{Tafel} (%)
Blank	1	453	1364	95.6	—
PPB	10^{-3}	469	120	67.3	91.2
	10^{-4}	462	325	70.8	76.1
	10^{-5}	477	465	65.9	65.9
	10^{-6}	483	930	72.8	31.8

It is clear from the electrochemical polarisation results that the addition of inhibitor causes a decrease of the current density. The values I_{corr} of carbon steel in the inhibited solution are smaller than those for the inhibitor free solution (Table 1). The parallel cathodic Tafel plots obtained in Fig. 2 indicate that the hydrogen evolution is activation-controlled and the reduction mechanism is not affected by the presence of inhibitor. The anodic branches are slightly affected in the presence of this inhibitor. However, a shift of corrosion potential (E_{corr}) towards cathodic side i.e -453 to -483 mV was established. In literature, [24] it has been reported that (i) if the displacement in E_{corr} is >85 mV with respect to E_{corr} , the inhibitor can be seen as a cathodic or anodic type and (ii) if displacement in E_{corr} is <85 , the inhibitor can be seen as mixed type. In the present study, shift in E_{corr} values is in the range of 9-30 mV, so we can classify our inhibitor as mixed inhibitor with predominant cathodic effectiveness. Adsorption is the mechanism that is generally accepted to explain the inhibitory action of organic corrosion inhibitors. The adsorption of inhibitors can affect the corrosion rate in two ways: (i) by decreasing the available reaction area, i.e., the so-called geometric blocking effect, and (ii) by modifying the activation energy of the cathodic and/or anodic reactions occurring in the inhibitor-free metal in the course of the inhibited corrosion process. It is a difficult task to determine which aspects of the inhibiting effect are connected to the geometric blocking action and which are connected to the energy effect.

3.1.2. Effect of temperature

The temperature can modify the interaction between the carbon steel electrode surface and the acidic solution without and with inhibitor. The potentiodynamic polarization curves of carbon steel in 1M HCl with and

without 10^{-3} M of PPB at the temperature range from 298 to 328 K are shown in fig.3. The various electrochemical parameters were calculated from the Tafel plots and summarized in table 2. The inhibition efficiency is also presented in this table.

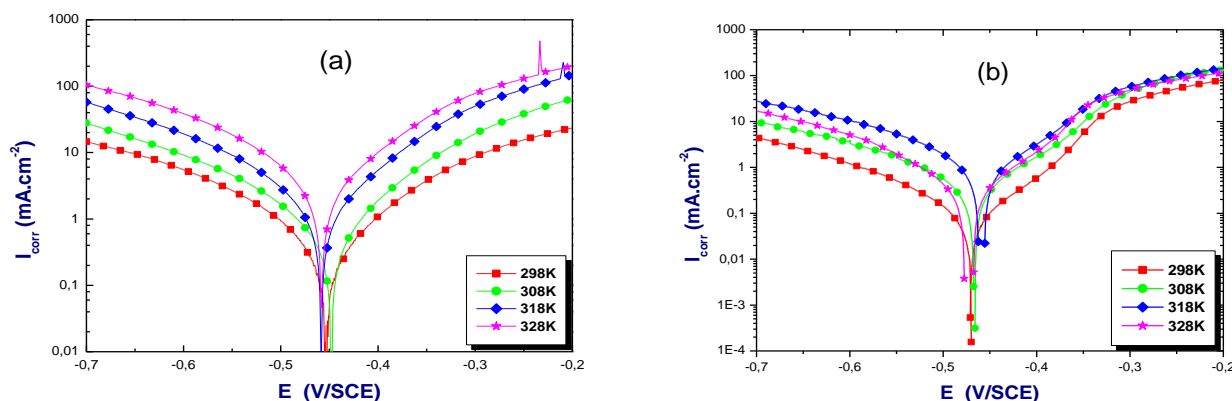


Figure 3: Potentiodynamic polarization curves of carbon steel in 1M HCl at different temperatures without (a) and with 10^{-3} M of PPB (b).

Table 2: The influence of temperature on the electrochemical parameters for carbon steel in 1M HCl and 10^{-3} M PPB

Medium	Temp (K)	$-E_{corr}$ (mV/SCE)	I_{corr} ($\mu\text{A}/\text{cm}^2$)	$-\beta_c$ (mV/dec)	η_{Tafel} (%)
Blank	298	453	1364	95.6	—
	308	448	1715	106.1	—
	318	457	2266	102.5	—
	328	457	2704	100.3	—
PPB	298	469	120	67.3	91.2
	308	467	282	70.8	83.5
	318	461	514	66.7	77.3
	328	476	930	69.6	65.6

It can be seen from Table 2 that the current corrosion density increased with increasing temperature both in uninhibited and inhibited solutions and the values of inhibition efficiency of PPB decreased with increasing temperature range studied.

To calculate activation parameters of the corrosion process, Arrhenius Eq. (3) and transition state Eq. (4) were used:

$$I_{corr} = A \exp\left(-\frac{E_a}{RT}\right) \quad (3)$$

$$I_{corr} = \frac{RT}{Nh} \exp\left(\frac{\Delta S_a}{R}\right) \exp\left(\frac{\Delta H_a}{RT}\right) \quad (4)$$

where E_a is the apparent activation corrosion energy, R is the universal gas constant, A is the Arrhenius pre-exponential factor, h is Plank's constant, T is the absolute temperature, ΔS_a is the entropy of activation and ΔH_a is the enthalpy of activation.

The apparent activation energies (E_a) in the absence and in the presence of various concentrations of PPB are calculated by linear regression between $\ln(I_{corr})$ and $1/T$ (Figure 4), and the results are given in Table 3. As observed from Table 3, the increase of E_a in the presence of of PPB. The increase in E_a in the presence of PPB may be interpreted as physical adsorption. Indeed, a higher energy barrier for the corrosion process in the inhibited solution is associated with physical adsorption or weak chemical bonding between the inhibitor species and the steel surface [25,26]. Szauer and Brand explained that the increase in activation energy can be attributed to an appreciable decrease in the adsorption of the inhibitor on the carbon steel surface with the increase in

temperature. A corresponding increase in the corrosion rate occurs because of the greater area of metal that is consequently exposed to the acid environment [27].

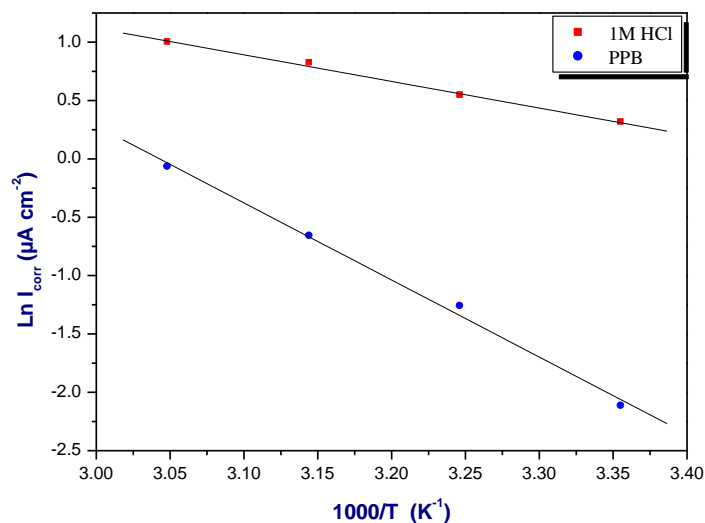


Figure 4: Arrhenius plots for carbon steel in 1 M HCl in the absence and presence of 10^{-3} M of PPB at different temperature.

Fig. 5 shows a plot of $\ln(I_{\text{corr}}/T)$ against $1000/T$, with a slope of $(\Delta H_a/R)$ and an intersection of $(\ln R/Nh + \Delta S_a/R)$ from which the values of ΔH_a and ΔS_a are calculated and listed in Table 3.

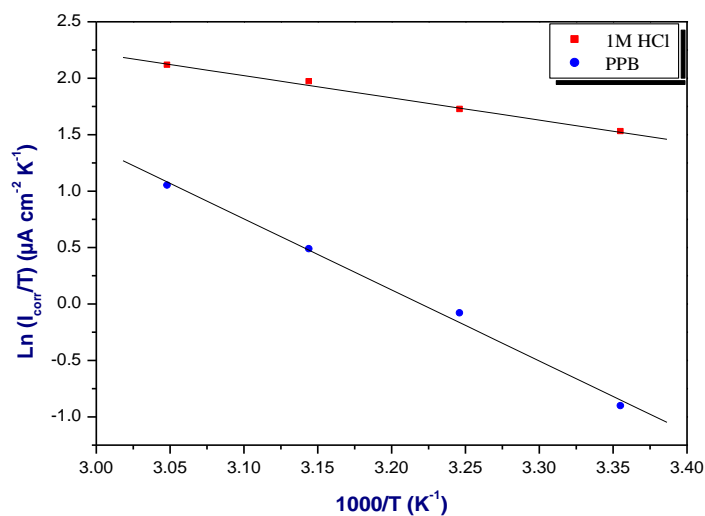


Figure 5: Transition Arrhenius plots for carbon steel in 1M HCl in the absence and presence of 10^{-3} M of PPB at different temperature.

The positive values of ΔH_a in the absence and the presence of PPB reflect the endothermic nature of the carbon steel dissolution process. In addition, the value of ΔS_a is higher for inhibited solutions than that for the uninhibited solution (Table 3). This suggested that an increase in randomness occurred on going from reactants to the activated complex. This might be the results of the adsorption of organic inhibitor molecules from the nitric solution could be regarded as a quasi-substitution process between the organic compound in the aqueous phase and water molecules at electrode surface [28]. In this situation, the adsorption of organic inhibitor was accompanied by desorption of water molecules from the surface. Thus the increasing in entropy of activation was attributed to the increasing in solvent entropy [29].

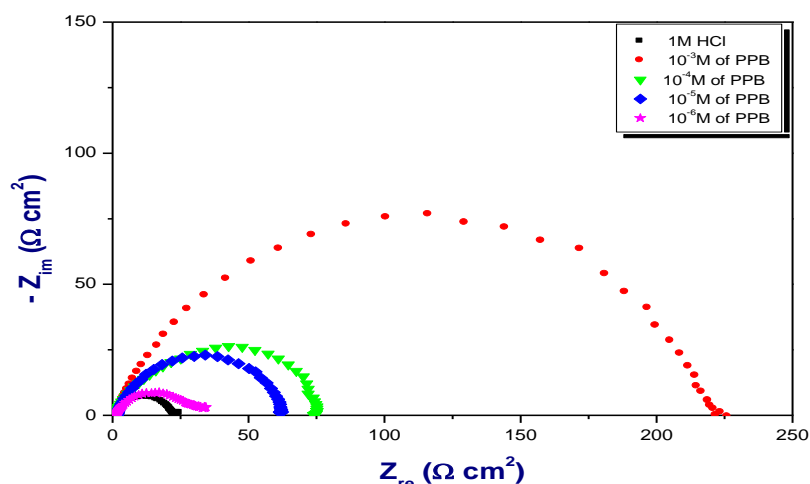
Table 3: the values of activation parameters in the presence and the absence of PPB

Medium	E_a (KJ/mol)	ΔH_a (KJ mol ⁻¹)	ΔS_a (J mol ⁻¹ K ⁻¹)
Blank	18.9	16.4	-141.9
PPB	54.9	52.3	-41.0

3.2. Electrochemical impedance spectroscopy

3.2.1. Effect of concentration

The representative Nyquist plots of carbon steel in 1M HCl solution in the absence and presence of various concentrations of PPB is shown in Fig.6 after immersion for 30 min at 298 K. The parameters associated with the diagram impedance such as charge transfer resistance R_{ct} , double layer capacitance C_{dl} , maximum frequency f_{max} and efficiency inhibition are presented in table 4. Clearly, the impedance spectra exhibit a large capacitive loop at high frequencies. The capacitive loop indicates that the corrosion of steel is mainly controlled by a charge transfer process [30,31], and usually related to the charge transfer of the corrosion process and double-layer behavior. The diameter of the capacitive loop in the presence of the inhibitor is larger than in the absence of the inhibitor (blank solution) and increases with the inhibitor concentration. This indicates that the impedance of inhibited substrate increases with the inhibitor concentration. Noticeably, these capacitive loops are not perfect semicircles which can be attributed to the frequency dispersion effect. This anomalous behavior is generally attributed to the roughness and inhomogeneity of the metal surface [32].

**Figure 6:** Nyquist diagram of carbon steel in 1M HCl without and with different concentrations of PPB.**Table 4:** Corrosion parameters obtained from impedance measurements of carbon steel in 1M HCl containing various concentrations of PPB at 298 K.

Medium	Conc (M)	R_{ct} (Ω cm ²)	C_{dl} (μ F cm ⁻²)	f_{max} (Hz)	η_z (%)
Blank	1	20.4	156.1	50	—
PPB	10^{-3}	220.5	72.2	10	90.7
	10^{-4}	82.6	96.4	20	75.3
	10^{-5}	61.2	130.1	20	66.6
	10^{-6}	29.5	215.9	25	30.8

The opposite trend in the values of R_{ct} and C_{dl} (Table 1) at the whole concentration range, it can be supposed that a protective layer covers the whole surface of the electrode. The double layer between charged metal surface and the solution is considered as an electrical double capacitor. The adsorption of this inhibitor on the carbon steel surface decreases its electrical capacity because of the displacement of water molecule and other ions originally adsorbed on the metal surface. The decrease in this capacity with increase in inhibitory

concentration may be attributed to the formation of a protective film on the electrode surface [33]. The thickness of this protective layer increases with increase in inhibitor concentration, as more benzenamine derivative electro statically adsorbed on the electrode surface, resulting in a noticeable decrease in C_{dl} . This trend is in accordance with Helmholtz model given by the equation

$$C_{dl} = \frac{\epsilon\epsilon_0 A}{d} \quad (5)$$

where ϵ_0 is the vacuum dielectric constant, ϵ is the local dielectric constant, d is the thickness of the double layer, and A is the surface area of the electrode.

3.2.2. Adsorption Isotherm:

The adsorption of inhibitor on the metal / solution interface is a substitution process, in which the water molecules adsorbed on the metal surfaces are replaced by the inhibitory molecules. According to the following equation [34,35]:



where x , the size ratio, is the number of water molecules displaced by one molecule of organic inhibitor. x is assumed to be independent of coverage or charge on the electrode.

Several adsorption isotherms were evaluated. And the Langmuir adsorption isotherm proved to be the best description of the adsorption behavior of the inhibitor studied. It may be expressed by the following equation (7) [36]:

$$\frac{C_{inh}}{\theta} = \frac{1}{K_{ads}} + C_{inh} \quad (7)$$

where C_{inh} is the equilibrium inhibitor concentration, K_{ads} adsorptive equilibrium constant, representing the degree of adsorption i.e., the higher the value of K_{ads} indicates that the inhibitor is strongly adsorbed on the metal surface.

The plot of C_{inh}/θ versus C yields a straight line with a slope close to 1 and the linear association coefficient (R^2) is also nearly 1, as shown in Fig.7, indicating that the adsorption of PPB on the carbon steel surface obeys Langmuir adsorption isotherm. The standard free energy of adsorption (ΔG_{ads}°) was calculated by using the following expression (Eq. 8) [37].

$$\Delta G_{ads}^\circ = -RTL \ln(55.5K_{ads}) \quad (8)$$

where R is the universal gas constant, 55.5 is the concentration of water in solution and T (K) is the thermodynamic temperature. The calculated values of ΔG_{ads}° and K_{ads} for PPB are regrouped in Table 5.

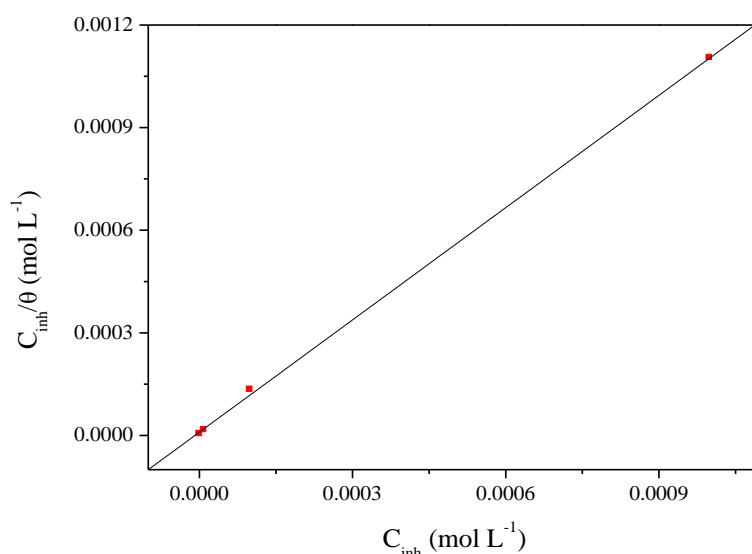


Figure 7: Langmuir adsorption of inhibitor on the carbon steel surface in 1M HCl solution at 298K.

Table 5: Adsorption parameters of inhibitor for carbon steel corrosion in 1 M HCl at 298 K.

Inhibitor	Slope	R ²	K _{ads} (M ⁻¹)	-ΔG _{ads} ^o (KJ/mol)
PPB	1.09	0.99983	106209.4	38.62

Generally, if the absolute values of ΔG_{ads}° are less than 20 kJ mol⁻¹ consistent with the electrostatic interaction between the charged metal and charged molecules (physisorption), but if those more than 40 kJ mol⁻¹ involve sharing or transfer of electrons from the inhibitor compound to the metal surface to form a co-ordinate type of bond (chemisorption) [38,39]. The value of ΔG_{ads}° calculated in this study is less than 20 kJ mol⁻¹ (ΔG_{ads}° (-38.62 kJ mol⁻¹) this value can be suggested that the interaction of the PPB involves both physisorption and chemisorptions [40].

3.3. Theoretical calculations

To study the effect of molecular structure on the inhibition mechanism some quantum chemical calculations have been performed. The optimized molecular structure of PPB is presented in Fig.8 and the frontier molecule orbital density distributions of PPB were presented in Fig.9. The Quantum chemical parameters such as E_{HOMO} , E_{LUMO} , $\Delta E = (E_{LUMO} - E_{HOMO})$, softness (σ), the fraction of electrons transferred (ΔN) and dipole moment (μ) were collected in Table 6.

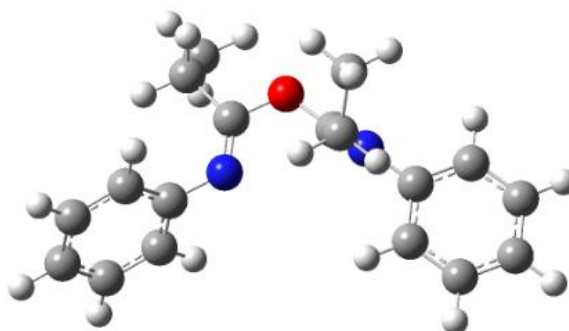


Figure 8: Optimized structure of the studied molecule obtained by B3LYP/6-31G(d,p) method.

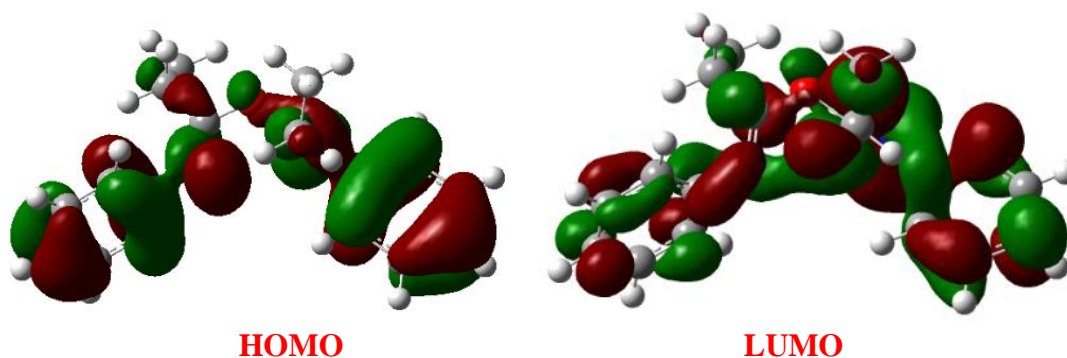


Figure 9: Frontier molecule orbital density distributions of the synthesized inhibitor.

In Fig. 9, the HOMO and LUMO orbitals are distributed over the entire molecule, resulting in the strongest interaction of the inhibitor on the carbon steel surface. This observation also suggests that heteroatoms and aromatic rings containing π bonds are probable reactive sites for the adsorption of inhibitor on the metal surface. E_{HOMO} is a quantum chemical parameter that is associated with the ability to offer electrons to the molecule; This capacity becomes larger with a high value of E_{HOMO} . In other case, E_{LUMO} indicates the ability of the molecule to accept electrons [41,42]. The difference between the HOMO and LUMO energies (ΔE) gives an indication of the chemical reactivity of a molecule. The inhibitor with a small ΔE should exhibit a higher interaction with the metal surface.

The absolute electronegativity (χ), global hardness (η) and global softness (σ) of the inhibitor molecule are approximated as follows [43,44]:

$$\chi = \frac{IE + EA}{2} \quad (9)$$

$$\eta = \frac{IE - EA}{2} \quad (10)$$

$$\sigma = \frac{1}{\eta} \quad (11)$$

Where the ionization potential (I) and the electron affinity (A) are defined as follows Eqs:12,13:

$$I = -E_{\text{HOMO}} \quad (12)$$

$$A = -E_{\text{LUMO}} \quad (13)$$

Thus the fraction of electrons transferred from the inhibitor to metallic surface, ΔN , is given by following eq. [45]:

$$\Delta N = \frac{\chi_{\text{Fe}} - \chi_{\text{inh}}}{2(\eta_{\text{Fe}} + \eta_{\text{inh}})} \quad (14)$$

where χ_{Fe} and χ_{inh} denote the absolute electronegativity of iron and inhibitor molecule η_{Fe} and η_{inh} denote the absolute hardness of iron and the inhibitor molecule respectively. In this study, we use the theoretical value of $\chi_{\text{Fe}} = 7.0$ eV and $\eta_{\text{Fe}} = 0$, for calculating the number of electron transferred.

The Table 6 present the parameters obtained by DFT calculation method. This research proposes that the inhibition efficiency increases with increasing softness and decreases on increasing the hardness of the inhibitor molecules.

Table 6: the quantum chemical parameters of PPB calculated using DFT at the highest (B3LYP/6-31G (d, p)) level.

Parameters	E_{HOMO} (eV)	E_{LUMO} (eV)	ΔE_{gap} (eV)	η (eV)	σ (eV ⁻¹)	χ (eV)	ΔN	μ (D)
PPB	-5.861	-0.455	5.406	2.703	0.369	3.158	0.710	1.926

Frontier orbital theory was useful in predicting the adsorption centers of the inhibitor molecule PPB responsible for its interaction with surface metal atoms [46]. Terms involving the frontier molecular orbital could provide a dominative contribution because of the inverse dependence of stabilization energy on orbital energy difference. Excellent corrosion inhibitors are usually organic compounds that not only offer electrons to unoccupied orbitals of the metal but also accept free electrons from the metal [47]. A relationship between the corrosion inhibition efficiency of the synthesized compound with the orbital energies of the HOMO (E_{HOMO}) and LUMO (E_{LUMO}) as well as the dipole moment (μ) are shown in Table 6. As is clearly observed in the Table 6, the inhibition efficiency increases with an increase in E_{HOMO} values along with a decrease in E_{LUMO} values.

The E_{HOMO} is often associated with the electron donating ability of a molecule. Therefore, increasing values of E_{HOMO} indicate a higher tendency for the donation of electron(s) to the appropriate acceptor molecule with low energy and an empty molecular orbital. Increasing values of E_{HOMO} thus facilitate the adsorption of the inhibitor. Consequently, improving the transport process through the adsorbed layer would enhance the inhibition efficiency of the inhibitor. This finding can be explained as follows. E_{LUMO} indicates the ability of the molecule to accept electrons; therefore, a lower value of E_{LUMO} more clearly indicates that the molecule would accept electrons [48]. The dipole moment (μ) is an index that can also be used to predict the direction of a corrosion inhibition process. Dipole moment is the measure of polarity in a bond and is related to the distribution of electrons in a molecule. Although literature is inconsistent on the use of μ as a predictor of the direction of a corrosion inhibition reaction, it is generally agreed that the adsorption of polar compounds possessing high dipole moments on the metal surface should lead to better inhibition efficiency. The data obtained from the present study indicate that the PPB inhibitor has the value of $\mu = 1.926$ D and highest inhibition efficiency (91%). The dipole moment is another indicator of the electronic distribution within a molecule. Some authors state that the inhibition efficiency increases with increasing values of the dipole moment, which depends on the type and nature of molecules considered. However, there is a lack of agreement in the literature on the

correlation between μ and % IE, as in some cases no significant relationship between these values has been identified [49,50].

The number of electrons transferred (ΔN) was also calculated and tabulated in Table 6. Generally, value of ΔN shows inhibition efficiency resulting from electron donation, and the inhibition efficiency increases with the increase in electron-donating ability to the metal surface. Value of ΔN show inhibition effect resulted from electrons donation. According to Lukovits's study [51], if $\Delta N < 3.6$, the inhibition efficiency increases with increasing electron-donating ability at the metal surface. Based on these calculations, it is expected that the synthesized inhibitor is donor of electrons, and the steel surface is the acceptor, and this favors chemical adsorption of the inhibitor on the electrode surface. Here the inhibitor binds to the steel surface and forms an adsorption layer against corrosion.

Conclusion:

From the experimental and theoretical part, the following conclusions can be drawn:

- From the results obtained we can be concluded that PPB exposed good inhibiting properties for carbon steel corrosion in 1M HCl solution and increased with increasing the concentration of inhibitor but decreases with temperature.
- Polarization studies showed that the studied inhibitor act as mixed inhibitor.
- EIS measurement results indicate that the resistance of the carbon steel increases greatly and the double layer capacitance (C_{dl}) decreases by increasing the inhibitor concentration.
- The adsorption of the inhibitor on carbon steel surface obeys the Langmuir adsorption isotherm.
- Quantum chemical calculation by DFT method were performed to identify the reactivity of tested molecule towards corrosion inhibition and the results are in good agreement with the experimental studies .

Référence:

1. Ben Hmamou D., Salghi R., Zarrouk A., Zarrok H., Hammouti B., Al-Deyab S. S., El Assyry A., Benchat N., Bouachrine M. *Int. J. Electrochem. Sci.*, 8 (2013) 11526 .
2. Ait Albrimi Y., Ait Addi A., Douch J., Hamdani M., Souto R.M. *Int. J. Electrochem. Sci.*, 11 (2016) 385 .
3. Shahabi S., Norouzi P., Ganjali M. R. *Int. J. Electrochem. Sci.*, 10 (2015) 2646 – 2662.
4. Benbouya K., Zerga B., Sfaira M., Taleb M., Ebn Touhami M., Hammouti B., Benzeid H., Essassi E.M. *Int. J. Electrochem. Sci.*, 7 (2012) 6313.
5. Quraishi M.A., Rawat J., *Mater. Chem. Phys.* 77 (2002) 43.
6. Nazeera Banua V.R., Rajendranb S., Senthil Kumaran S., *J. Alloys Compd.* 675 (2016) 139.
7. Bouklah M., Ouassini A., Hammouti B., El Idrissi A., *Appl. Surf. Sci.* 250 (2005) 50-56
8. Vracar L.M., Drazic D.M., *Corros. Sci.* 44 (2002) 1669.
9. Bouklah M., Hammouti B., Aouniti A., Benhadda T., *Prop. Org. Coat.* 47 (2004) 225.
10. Bouzidi D., Kertit S., Hammouti B., Brighli M., *J. Electrochem. Soc. India* 46(1997) 23.
11. Martinez S., Stern I., *Appl. Surf. Sci.* 199 (2002) 83.
12. Ghazoui A., Zarrouk A., Bencat N., Salghi R., Assouag M., El Hezzat M., Guenbour A., Hammouti B., *J. Chem. Pharm. Res.* 6 (2014) 704.
13. Zarrok H., Zarrouk A., Salghi R., Ramli Y., Hammouti B., Al-Deyab S.S., Essassi E.M., Oudda H., *Int. J. Electrochem. Sci.* 7(9) (2012) 8958.
14. Bendaha H., Zarrouk A., Aouniti A., Hammouti B., El Kadiri S., Salghi R., Touzan R., *Phys. Chem. News* 64 (2012) 95.
15. Zarrouk A., Hammouti B., Zarrok H., Salghi R., Dafali A., Bazzi L., Bammou L., Al-Deyab S.S., *Der Pharm. Chem.* 4(1) (2012) 337.
16. Ghazoui A., Saddik R., Benchat N., Hammouti B., Guenbour M., Zarrouk A., Ramdani M., *Der Pharm. Chem.* 4(1) (2012) 352.
17. Zarrouk A., Hammouti B., Zarrok H., Bouachrine M., Khaled K.F., Al-Deyab S.S., *Int. J. Electrochem. Sci.* 6 (2012) 89.
18. Zarrok H., Zarrouk A., Salghi R., Assouag M., Hammouti B., Oudda H., Boukhris S., Al Deyab S.S., Warad I., *Der Pharm. Lett.* 5 (2013) 43.
19. Zarrok H., Saddik R., Oudda H., Hammouti B., El Midaoui A., Zarrouk A., Benchat N., Ebn Touhami M., *Der Pharm. Chem.* 3(5) 2011) 272.

20. Zarrouk A., Hammouti B., Touzani R., Al-Deyab S.S., Zertoubi M., Dafali A., Elkadiri S., *Int. J. Electrochem. Sci.* 6 (10) (2011) 4939.
21. McCafferty E., Leidheiser H. (Ed.), *Corrosion Control by Coating*, Science Press, Princeton, JJ, 1979, p. 279.
22. Frisch M.J., Trucks G.W., Schlegel H.B., Scuseria G.E., Robb M.A., GAUSSIAN 03, Revision B.04, Gaussian, Inc., Pittsburgh PA, 2003 and al.
23. Becke A.D., Density-functional thermochemistry. III. The role of exact exchange, *J. Chem. Phys.* 98 (1993) 5648.
24. El Faydy M., Galai M., El Assyry A., Tazouti A., Tourir R., Lakhrissi B., Ebn Touhami M., Zarrouk A., *J. Mol. Liq.* 219 (2016) 396.
25. Popova A., Sokolova E., Raicheva S., Christov M., *Corros. Sci.* 45 (2003) 33.
26. Li X., Mu G., *Appl. Surf. Sci.* 252 (2005) 1254.
27. Szauer T., Brandt A., *Electrochimica Acta* 26 (1981) 1219.
28. Zarrouk A., Hammouti B., Dafali A., Bentiss F., *Ind. Eng. Chem. Res.* 52 (2013) 2560.
29. Ateya B., El-Anadouli B.E., El-Nizamy F.M., *Corros. Sci.* 24 (1984) 509.
30. Ghazoui A., Benchat N., El-Hajjaji F., Taleb M., Rais Z., Saddik R., Elaattiaoui A., Hammouti B., *J. Alloys Compd.* 693 (2017) 510.
31. El ouasif L., Merimi I., Zarrok H., El ghoual M., Achour R., Guenbour M., Oudda H., El-Hajjaji F., Hammouti B., *J. Mater. Environ. Sci.* 7 (8) (2016) 2718.
32. Lebrini M., Lagrenée M., Vezin H., Traisnal M., Bentiss F., *Corros. Sci.* 49 (2009) 2254.
33. Lopez D.A., Simison S.N., de Sanchez S.R., *Electrochim. Acta* 48 (2003) 845.
34. Moretti G., Guidi F., Fabris F., *Corros. Sci.* 76 (2013) 206.
35. Kharchouf S., Majidi L., Bouklah M., Hammouti B., Bouyanzer A., Aouniti A., *Arab. J. Chem.* 7 (2014) 680.
36. Solmaz R., *Corros. Sci.* 81 (2014) 75.
37. Negm N.A., Elkholy Y.M., Zahran M.K., Tawfik S.M., *Corros. Sci.* 52 (2010) 3523.
38. Bentiss F., Lebrini M., Lagrenée M., *Corros. Sci.* 47 (2005) 2915.
39. Salim R., Ech Chihbi E., Oudda H., ELAoufir Y., El-Hajjaji F., Elaattiaoui A., Oussaid A., Hammouti B., Elmsellem H. and Taleb M., *Der Pharm. Chem.* 8 (13) (2016) 200.
40. Yang Z., Zhan F., Pan Y., LYu Z., Han C., Hu Y., Ding P., Gao T., Zhou X., Jiang Y., *Corros. Sci.* 99 (2015) 281.
41. Kalil N., *Electrochim. Acta.* 48 (2003) 2635–2640.
42. Rameshkumar S., Danae I., Rashvand Avei M., Vijayan M., *J. Mol. Liq.* 212 (2015) 168.
43. Eddy N.O., Momoh-Yahaya H., Oguzie E.E., *J. Adv. Res.* 6 (2015) 203.
44. Olasunkanmi L.O., Kabanda M.M., Ebenso E.E., *Phys E Low-Dimens Syst Nanostructures.* 76 (2016) 109.
45. Martinez S., *Mater. Phys.* 77 (2003) 97.
46. Kandemirli F., Sagdinc S., *Corros. Sci.* 49 (2007) 2118.
47. Al-Amiery A.A., Musa A.Y., Kadhun A.A.H., Mohamad A., *Molecules* 16 (2011) 6833.
48. Costa J.M., J.M. Lluch, *Corros. Sci.* 24 (1984) 924.
49. Khalil N., *Electrochim. Acta* 48 (2003) 2635.
50. Bereket G., Ogretir C., Yurt A., *J. Mol. Struct. (Theochem.)* 571 (2001) 139.
51. Lukovits I., Kalman E., Zucchi F., *Corrosion* 57 (2001) 3.

(2017) ; <http://www.jmaterenvironsci.com>